# Journal Pre-proof


A DNA-based biosensor for aqueous Hg(II): Performance under variable pH, temperature and competing ligand composition

Kunfu Pi, Juewen Liu, Philippe Van Cappellen

PII: S0304-3894(19)31526-2

DOI: https://doi.org/10.1016/j.jhazmat.2019.121572

Reference: HAZMAT 121572

To appear in: *Journal of Hazardous Materials*

Received Date: 5 July 2019

Revised Date: 4 October 2019

Accepted Date: 29 October 2019

Please cite this article as: Pi K, Liu J, Van Cappellen P, A DNA-based biosensor for aqueous Hg(II): Performance under variable pH, temperature and competing ligand composition, *Journal of Hazardous Materials* (2019), doi: https://doi.org/10.1016/j.jhazmat.2019.121572

# A DNA-based biosensor for aqueous Hg(II): Performance under variable pH, temperature and competing ligand composition

Kunfu Pi [a,*], Juewen Liu [b], Philippe Van Cappellen [a,*]

[a] *Ecohydrology Research Group, Department of Earth and Environmental Sciences & Water Institute, University of Waterloo, Waterloo, Ontario, N2L 3G1 Canada*

[b] *Department of Chemistry & Waterloo Institute for Nanotechnology, University of Waterloo, Waterloo, Ontario, N2L 3G1 Canada*

[*]Correspondence: kpi@uwaterloo.ca (K.P.); pvc@uwaterloo.ca (P.V.C.)

Graphical abstract

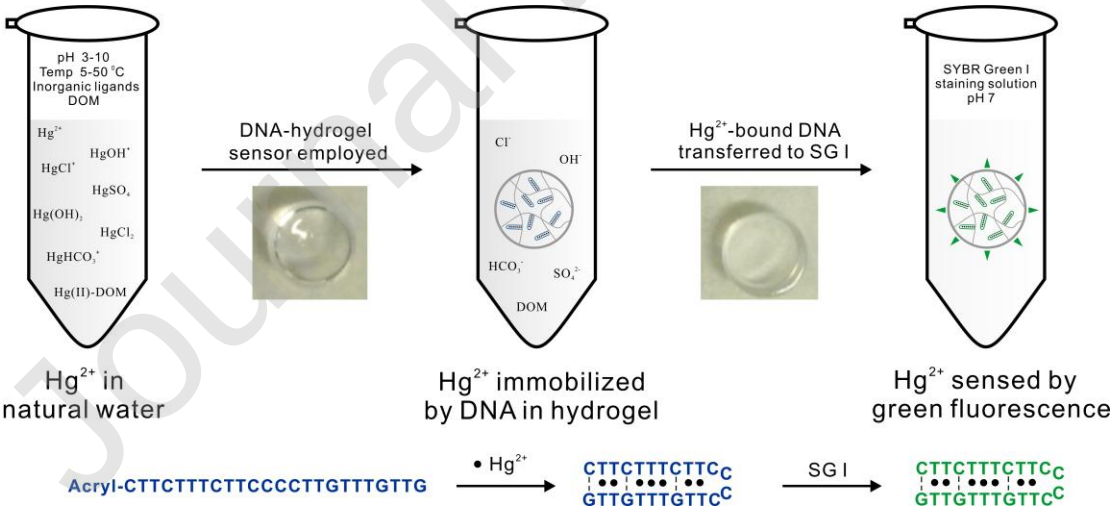


## Highlights

- A DNA biosensor for aqueous $Hg^{2+}$ is tested under environmentally relevant

conditions

- Solution interferences are reduced by incorporating the DNA molecules in hydrogel
- The temperature-dependent binding constant of $Hg^{2+}$ to the DNA sequence is derived
- Equilibrium calculations account for the competitive binding of $Hg^{2+}$ to NDOM

## Abstract

Mercury (Hg) is a toxic metal posing major health risks to human beings and wildlife. The characterization of Hg fate and transport in aquatic environments is hindered by a lack of sensitive, selective and easily field-deployable analytical techniques. Here we assess the reliability and performance of a $Hg^{2+}$ sensor based on the selective binding of $Hg^{2+}$ to a thymine-rich DNA under environmentally-relevant conditions. Experimental results indicate that the interactions between the DNA and SYBR Green I, which produce the detection fluorescence signal, are significantly impacted by pH, metal ligands and natural dissolved organic matter (NDOM). These interferences are largely eliminated by immobilizing the DNA in a polyacrylamide hydrogel, although high concentrations of NDOM, such as fulvic acids, still affect the sensor's performance due to competitive binding of $Hg^{2+}$. The binding of $Hg^{2+}$ to NDOM, however, can be accounted for via equilibrium speciation calculations, which also yield the complexation constant for $Hg^{2+}$ binding to the DNA in the hydrogel. The

equilibrium calculations reproduce the results for the entire set of experimental conditions, from simple electrolyte solutions to complex aqueous compositions mimicking natural lake waters, and across large ranges of pH (3-10) and temperature (5-50 ˚C).

**Keywords**: Mercury; Environmental monitoring; Biosensor; DNA-functionalized hydrogel; Dissolved organic matter

## 1. Introduction

Mercury (Hg) is a toxic metal and global pollutant [1-3] that poses severe health risks to humans and wildlife [4,5]. Awareness of the dangers of Hg has resulted in substantial efforts to control anthropogenic emissions, yet historical Hg legacies and geogenic sources still pose significant long-term threats [6-8]. Together with inorganic $Hg^{+}$ and methylmercury, oxidized inorganic $Hg^{2+}$ is considered a main concern for drinking water safety and consequently a major focus in source water quality monitoring and protection [9]. Moreover, research on the biogeochemical cycling and transport of Hg in aquatic environments, as well as the management and remediation of Hg pollution, stands to benefit from analytical methods that allow for the rapid, in-situ detection of aqueous $Hg^{2+}$ [5,10,11].

Currently, aqueous Hg analyses mainly rely on atomic emission spectroscopy [12,13], atomic fluorescence spectrometry [14,15], inductively coupled plasma mass

spectrometry [16,17], and electrochemical methods [18,19]. These methods require sizable instruments and supporting facilities operated under well-controlled laboratory conditions and, in most cases, only yield total aqueous Hg concentrations. These methods are therefore difficult to deploy directly in the field, especially at remote locations. They are also time-consuming and costly, and usually produce hazardous wastes that must be carefully disposed. In addition, they may not provide information about aqueous Hg speciation, which controls mercury mobility and toxicity [1,4,7].

The limitations of traditional instrumental methods open opportunities for alternative analytical techniques that are fast, flexible, portable, and user-friendly. In recent years, researchers have developed different types of DNA-based Hg sensors that have the potential to meet the above criteria [20-30]. One approach that is highly specific to aqueous $Hg^{2+}$ is based on $Hg^{2+}$-mediated thymine-thymine DNA base-pairing [25,31,32], which folds a single-stranded DNA molecule into a hairpin structure. The duplex structure can enhance fluorescence emission upon the addition of a DNA staining dye, for example SYBR Green I [20,26,33], quench the fluorescent emission via fluorescence resonance energy transfer [27], or induce signal shifts during its adsorption to nanomaterials [28-30].

Because only $Hg^{2+}$ stabilizes the thymine-thymine base pair, without similar responses triggered by other cations known to bind to nucleic acids (e.g., $Ag^{+}$, $Cu^{2+}$, $Fe^{3+}$), this unique interaction has enabled the development of $Hg^{2+}$-specific biosensors [20,26,28,30,33]. Furthermore, the thymine-rich DNA sequences can be incorporated

into hydrogels to form a portable sensor that has the potential to detect $Hg^{2+}$ with a high sensitivity (≤10 nM) in natural waters [20,34,35]. Such hydrogels thus provide a promising support material for the development of environmental biosensors for aqueous $Hg^{2+}$ and other toxic metals.

Although the concept of DNA-based biosensors has been demonstrated in "clean" laboratory aqueous media with stable buffers [20,24,25,34], variable pH and temperature, and the presence of inorganic ligands, colloids and natural dissolved organic matter (NDOM) in aquatic environments all potentially alter the interactions between $Hg^{2+}$ and the DNA, as well as between the DNA and the staining dye [36-39]. Before the DNA-based biosensors are deployed in the field, a better characterization of their sensitivity and stability and a quantitative understanding of the potential environmental interferences on their performance are required.

In this study, we examine the performance of a DNA-based $Hg^{2+}$ fluorescence sensor as a function of pH, temperature, and the presence of inorganic ligands and NDOM. We compare the detection capacity of the selected DNA sequence both in solution and after incorporation in a hydrogel. The results are interpreted using thermodynamic equilibrium calculations that account for the competitive binding of $Hg^{2+}$ to the DNA molecules, the inorganic ligands and NDOM, and for the temperature-dependent $Hg^{2+}$-DNA complexation. The results support the feasibility of applying the DNA-based $Hg^{2+}$ sensor technology in freshwater environments.

## 2. Materials and methods

### 2.1. Sensor preparation

The single-stranded DNA (Acryl-5′-CTTCTTTCTTCCCCTTGTTTGTTG) was purchased from Integrated DNA Technologies (Coralville, USA). For the solution-based DNA experiments (Table 1), the aqueous compositions were assembled in Milli-Q water (18.2 MΩ·cm) prior to the addition of variable volumes of 1 mg $L^{-1}$ $Hg^{2+}$ standard solution prepared from a 1000 mg $L^{-1}$ $Hg^{2+}$ stock solution ($Hg(ClO_4)_2$ in $H_2O$, Delta Scientific, Canada). As representative NDOM, Suwannee River Fulvic Acid (SRFA, International Humic Substance Society) was used because of its well-characterized chemical properties and the prevalence of fulvic acids in freshwaters [40-42].

The DNA-functionalized polyacrylamide hydrogels were prepared in 96-well clear microplates [20]. The hydrogel preparation was carried out in pH 7 Tris-$NO_3$ buffer solutions (See Supplementary Material for details). On average, 45% of the added DNA was incorporated into the hydrogel, yielding a final DNA content in the hydrogel of ~3 μM. Hydrogels without DNA were also prepared and used as controls in each series of experiments.

### 2.2. Performance assessment

In the solution-based DNA experiments, a series of solutions containing the same DNA concentration but variable $Hg^{2+}$ concentrations were first used to derive a

calibration curve, with a detection limit of 10 nM $Hg^{2+}$ (Exp. S-I, Table 1). Next, the effects of pH, individual inorganic ligands ($Cl^-$, $SO_4^{2-}$, $HCO_3^-$, $H_2PO_4^-$) and SRFA on the fluorescence intensity were examined. For the variable pH experiments (Exp. S-II, Table 1), solutions of constant $Hg^{2+}$ concentration (90 nM) were prepared using two different sets of pH buffers for comparison (see footnote *a* in Table 1).

For the competitive ligand series, individual inorganic ligands and SRFA, with concentration ranges representative of those commonly observed in uncontaminated freshwaters [43,44], were added during the DNA-SYBR Green I solution preparation (Exp. S-III to S-VII, Table 1). The solution pH was kept constant at 7 using 8 mM Tris-$NO_3$, except for the experiments with $HCO_3^-$ where pH was 8. All the solutions were well mixed and left statically to react for 10 minutes at 25 ˚C prior to measuring the fluorescence on a Multimode Reader (Infinite 200Pro) equipped with 96-well clear-bottom microplates, at the excitation/emission wavelength of 485/535 nm. Controls without DNA were carried out in parallel.

In the DNA-functionalized hydrogel experiments, a calibration curve was first obtained at pH 7 (8 mM Tris-$NO_3$) and 25 ˚C using a series of variable $Hg^{2+}$ solutions (10-500 nM, Exp. G-I, Table 1) [20]. Next, the DNA-functionalized hydrogels were soaked for one hour in 1 mL of 100 nM $Hg^{2+}$ solution at variable pH (3-10), concentrations of inorganic ligands or SRFA, and temperature (5-50 ˚C) (Exp. G-II to G-VIII, Table 1) (See Supplementary Material for more information). Thereafter, the hydrogels were retrieved and washed twice with Milli-Q water, each time for 30

minutes. Next, the hydrogels were soaked in 1 mL of 610 nM SYBR Green I solution for 1 hour at 25 °C, then retrieved, cleansed of residual solution on the hydrogel surface, and imaged using a gel documentation system (Alpha Innotech FluorChem FC2) at the excitation wavelength of 365 nm, with a detection limit of 10 nM total $Hg^{2+}$.

In a final set of experiments with the DNA-functionalized hydrogels (Exp. G-IX and G-X, Table 1), artificial surface waters (ASW) were prepared mimicking the major hydrochemistry and pH conditions of the Laurentian Great Lakes [44-46] (Table 2). The ASW samples were spiked with $Hg^{2+}$ to a final concentration of either 50 or 100 nM. For each of the Great Lakes analogs, two types of ASW were prepared: (1) major inorganic cations, inorganic anions and pH reported for the corresponding lake (hereafter referred to as ASW-I), and (2) same inorganic compositions as ASW-I plus 10 mg DOC $L^{-1}$ of SRFA (hereafter referred to as ASW-II). These multicomponent ligand experiments were designed as a first step toward assessing the potential interferences on the performance of DNA-based $Hg^{2+}$ sensors in complex freshwater compositions.

All solution-based DNA and DNA-hydrogel experiments were conducted in triplicate. Mercury recoveries were assessed by adding the amounts of $Hg^{2+}$ immobilized in the hydrogel and the residual $Hg^{2+}$ concentrations in solution measured by the voltammetry method (see Supplementary Material for details), and compared with the amounts of $Hg^{2+}$ originally added. Recoveries across the experiments were 98±3%.

### 2.3. Equilibrium calculations

The aqueous speciation of $Hg^{2+}$ depends on pH [36] and the formation of complexes with inorganic ligands and NDOM [37,47]. The complexation of $Hg^{2+}$ with the various functional groups of NDOM was described here by the Humic Ion-Binding Model VII, which employs a structured formulation of discrete, but chemically plausible, binding sites for protons and metals [48]. The equilibrium speciation calculations were performed with the CHEAQS Next code, which includes the Humic Ion-Binding Model VII and an up-to-date database for $Hg^{2+}$ complexation reactions [49].

The equilibrium constant describing the binding of $Hg^{2+}$ to the DNA was derived by fitting the experimental data with CHEAQS Next and checked for consistency across the various experimental series. As the CHEAQS Next code only applies to complexation reactions at 25 °C, the effects of temperature on the binding of $Hg^{2+}$ to DNA (Exp. G-VIII, Table 1) were evaluated with PHREEQC-3 [50], using the *wateq4f* database, which accounts for the temperature-dependent $Hg^{2+}$ complexation with inorganic ligands [51] (See Supplementary Material for a list of the $Hg^{2+}$ complexation reactions).

## 3. Results

### 3.1. Mercury(II) detection by solution DNA

The fluorescence of the DNA solutions with 90 nM $Hg^{2+}$ exhibited a strong pH

dependence across the range tested (3-10), with a pronounced and reproducible maximum response at pH 7 in both pH buffer series (Fig. 1A). The lowest pH of 3 led to the almost complete quenching of the fluorescence signals.

The added inorganic ligands and SFRA attenuated the fluorescence to variable extents (Fig. 1B-F). Attenuation was insignificant for $Cl^-$ concentrations below 10 mg $L^{-1}$, but the fluorescence intensity dropped by 5% between 10 and 50 mg $L^{-1}$ $Cl^-$, and by another 9% between 50 and 250 mg $L^{-1}$ (Fig. 1B). Similarly, fluorescence attenuation was insignificant at $SO_4^{2-}$ concentrations ≤10 mg $L^{-1}$ and then gradually increased with increasing $SO_4^{2-}$ concentration (Fig. 1C). The general trend for the $HCO_3^-$ solutions was similar to those of $Cl^-$ and $SO_4^{2-}$, with an approximately 10% fluorescence attenuation at 500 mg $L^{-1}$ $HCO_3^-$ (Fig. 1D). Note that the systematically lower fluorescence intensities in the $HCO_3^-$ solutions, compared to other inorganic ligand solutions, were due to the higher pH (8 vs. 7, Table 1). The addition of $H_2PO_4^-$ at pH 7 did not cause much fluorescence quenching, with only a 2% decline between 0.05 and 10 mg $L^{-1}$ $H_2PO_4^-$ (Fig. 1E). The presence of 0.1-1 mg DOC $L^{-1}$ SRFA led to insignificant changes in the fluorescence (Fig. 1F), with the intensities close to the (SRFA-free) calibration curve (Fig. S1A). At SRFA concentrations of 10 and 50 mg DOC $L^{-1}$, the fluorescence decreased by about 3 and 6%, respectively.

### 3.2. Mercury(II) detection by DNA-hydrogel

In the DNA-functionalized hydrogel experiments, no pH dependence of the fluorescence was observed between pH 4 and 10 (Fig. 2A). Over this entire range, the

fluorescence intensities coincided with that predicted for 100 nM $Hg^{2+}$ by the pH 7 calibration curve of the DNA-functionalized hydrogel (Fig. S1B). Only at pH 3, a small intensity drop of about 4% was observed relative to the pH 7 fluorescence (Fig. 2A).

The presence of the inorganic ligands mostly caused little change in the DNA-hydrogel fluorescence (Fig. 2B-E). The largest attenuation occurred for $Cl^-$, where the intensity measured at 250 mg $L^{-1}$ was 4% lower than in the absence of $Cl^-$ (Fig. 2B). Moreover, the systematically lower fluorescence intensities in the pH 8 solution DNA series with added $HCO_3^-$ (Fig. 1D) were no longer observed in the corresponding DNA-hydrogel series (Fig. 2D). With increasing SRFA concentration, the DNA-hydrogel fluorescence decreased, resulting in almost 6% attenuation at 50 mg DOC $L^{-1}$ relative to SRFA-free conditions (Fig. 2F).

At pH 7 and 9, temperature variations in the range 5-50 ˚C had no impact on the fluorescence intensities of the DNA-functionalized hydrogels (Fig. 3). At pH 3, the fluorescence intensity at 5 ˚C was close to those of the corresponding pH 7 and 9 solutions, but it gradually decreased with increasing temperature, leading to a drop by 11% at 40 ˚C relative to 5 ˚C (Fig. 3A). In addition, the DNA-functionalized hydrogels were stable in the temperature range 5-50 ˚C, showing no visible shape change or other evidence of degradation.

### 3.3. Artificial lake surface waters

For the Laurentian Great Lakes analogs without SRFA (ASW-I, Table 2), the DNA-hydrogel fluorescence intensities mostly coincided with the values calculated at the corresponding $Hg^{2+}$ concentrations from the calibration curve (Fig. S1B). Only Lake Superior ASW-I solutions, which had the lowest pH of 6.3, exhibited slightly weaker fluorescence intensities relative to the ligand-free calibration solutions: 1.4% lower at 50 nM $Hg^{2+}$ and 2.8% at 100 nM $Hg^{2+}$ (Fig. 4A&B). With the exception of the Lake Superior analogs, the ASW-II samples, which contained an added 10 mg DOC $L^{-1}$ SRFA, exhibited comparable fluorescence intensities as their ASW-I counterparts (Fig. 4). For the Lake Superior ASW-II solutions, however, the intensities were 5.4% lower at 50 nM $Hg^{2+}$ and 8.4% lower at 100 nM $Hg^{2+}$.

### 3.4. Equilibrium calculations

The formation of the hairpin structure upon reaction between $Hg^{2+}$ and the DNA molecule involves the binding of $Hg^{2+}$ to two opposing thymine bases, which can be represented by the following chemical formula [20]:

$$2RNC_5H_4O_2NH + Hg^{2+} = Hg(RNC_5H_4O_2N)_2 + 2H^+ \qquad (1)$$

where $RNC_5H_4O_2NH$ represents the thymine base in the DNA molecules.

Fitting the DNA-hydrogel data from the variable pH experiments to the above reaction (Fig. 2A) yielded a complexation constant ($K_c$) at 25 °C of $10^{19.8}$. The large $K_c$ value implies that binding of $Hg^{2+}$ to the hydrogel-immobilized DNA molecules is highly favorable under the experimental conditions [31,32]. According to the

equilibrium calculations, in the ligand-free solutions at pH 3, the Hg(II)-DNA bridging complex accounted for ~80% of total $Hg^{2+}$, while the remaining 20% was made up almost entirely of aqueous $HgOH^+$ and $Hg(OH)_2$ complexes (Fig. 2A). For pH values from 4 to 10, the Hg(II)-DNA complex was the dominant $Hg^{2+}$ species, representing almost 100% of total $Hg^{2+}$.

With the above $K_c$ value, the fluorescence intensities of the individual ligand experiments at 25 ˚C are satisfactorily predicted by the equilibrium calculations (Fig. 2). The Hg(II)-DNA complex dominated $Hg^{2+}$ speciation in solutions with 0.5-50 mg $L^{-1}$ $Cl^-$ (Fig. 2B). At $Cl^-$ concentrations of 100 and 250 mg $L^{-1}$, $HgCl^+$ and HgClOH complexes together comprised 5.6 and 13% of total $Hg^{2+}$, respectively. For the other three inorganic ligands, the Hg(II)-DNA complex accounted for nearly 100% of total $Hg^{2+}$ across the ligand concentration ranges considered (Fig. 2C-E).

The equilibrium calculations further suggest that the Hg(II)-DNA complex dominated $Hg^{2+}$ speciation at SRFA concentrations up to 10 mg DOC $L^{-1}$ (Fig. 2F). At higher SRFA concentrations, Hg(II)-SRFA complexes, including $Hg(RCOO)_2$, HgRORCOO and $Hg(RO)_2$ (where R denotes the carbon backbone in the chemical formula), became increasingly important: at a concentration of 50 mg DOC $L^{-1}$, an estimated 33% of total $Hg^{2+}$ was bound to SRFA functional groups, with the remaining 67% of $Hg^{2+}$ complexed to the hydrogel-incorporated DNA (Fig. 2F).

The complexation constants for $Hg^{2+}$ binding to the DNA at different temperatures

were derived by fitting the data of Exp. G-VIII (Table 1), yielding a strong linear dependence of ln$K_c$ on reciprocal temperature between 278.15 and 323.15 K (5 and 50 ˚C) ($r^2$ = 0.9926, Fig. S2):

$$\ln K_c = 9775.2 \times \frac{1}{T} + 12.8 \qquad (2)$$

where $T$ is in Kelvin. According to the van't Hoff Equation, the linear relationship implies that the molar reaction enthalpy $\Delta H_m$ of the complexation reaction between $Hg^{2+}$ and the DNA can be treated as a constant value over the experimental temperature range, with a value of -81.27 kJ $mol^{-1}$.

At pH 7 and 9, the equilibrium calculations predict that $Hg^{2+}$ complexed with the hydrogel-incorporated DNA accounted for ~100% of total $Hg^{2+}$ at all temperatures between 5 and 50 ˚C (Fig. 3B&C). However, at pH 3 part of the $Hg^{2+}$ formed hydroxyl complexes and their relative importance increased with increasing temperature. As a result, compared to 5 ˚C, the observed fluorescence intensity was 11% lower at 40 ˚C (Fig. 3A).

The equilibrium calculations also well reproduce the results of the ASW-I and ASW-II solutions (Fig. 4). For ASW-I, the Hg(II)-DNA complex was the most important $Hg^{2+}$ species detected by the DNA-hydrogel sensor (Fig. 4A&B). The slight drop in fluorescence intensity for the Lake Superior analogs could be attributed to competing complexation of $Hg^{2+}$ with $Cl^-$, which was favored by the lower pH (6.3).

For the Lake Ontario ASW-II analog (pH 6.9), the Hg(II)-SRFA complexes represented 3.4% of total $Hg^{2+}$, very close to the 3.5% in the SRFA solutions with the same DOC concentration (10 mg DOC $L^{-1}$) in Exp. G-VII (compare Fig. 4D and 2F). In the higher pH ASW-II analogs of Lakes Michigan, Huron and East Erie, the Hg(II)-SRFA complexes accounted for less than 0.5% of total $Hg^{2+}$ (Fig. 4D). In Lake Superior ASW-II solutions with the lowest pH (6.3), the Hg(II)-SRFA complexes represented 54.3% of total $Hg^{2+}$. Therefore, with decreasing pH from 8.3 (Lake Huron) to 6.3 (Lake Superior), increasing Hg(II)-SRFA complexes formed for a constant SRFA concentration, regardless of the variations of inorganic ligands and cations in the ASW-II solutions.

## 4. Discussion

### 4.1. Performance of the solution-based DNA

Compared to the hydrogel-supported DNA, the fluorescence intensity of the solution-based DNA is much more vulnerable to variations in pH and the concentrations of competing inorganic ligands (compare the trends in Fig. 1A-E to those in Fig. 2A-E). Thus, the effects of pH and solution compositions observed in Fig. 1A-E cannot be solely due to variations in the aqueous speciation of $Hg^{2+}$. Most likely, the interferences of pH and inorganic ligands reflect effects on the interactions between the solution DNA and the SYBR Green I staining dye [52].

The hairpin structure formed upon addition of $Hg^{2+}$ induces the intercalation of SYBR Green I into the double-stranded region of the DNA molecule, which in turn dampens

the internal motion of the dye molecule and shifts the fluorescence emission from yellow to green [20,53]. Interactions with the phosphate groups of the DNA molecule bring about a stable conformation of SYBR Green I, leading to a substantial enhancement of the green fluorescence intensity [52]. In addition, the intercalation of the dye molecule favors contact of the elongated "arms" of the dye molecule via the positively charged amino groups with minor grooves of the double-stranded DNA, thereby enlarging the overall size of the binding site and consequently the fluorescence yield [26,52].

The above two forms of interactions between the double-stranded DNA and SYBR Green I are of electrostatic nature and are, therefore, sensitive to variations in pH and ionic strength [54]. Hence, the strong effect of pH on the fluorescence intensity (Exp. S-II, Table 1) can be ascribed to the disturbance of the electrostatic interactions between SYBR Green I and the phosphate groups of the DNA molecule. This interference is minimal at neutral pH but increases under both acidic and alkaline pH conditions. Note, however, that at pH 3 part of the fluorescence quenching also reflects the decreased extent of $Hg^{2+}$ complexation to DNA, as implied by the results of the DNA-hydrogel sensor tests under variable pH conditions (Fig. 2A).

The effects of the inorganic ligands on the measured fluorescence in the solution-based DNA experiments (Exp. S-III to S-VI, Table 1) can be linked to the ionic strength variations of the experimental solutions, irrespective of the different salts used (Fig. 5). The systematically lower exponential relationship between

fluorescence and ionic strength for bicarbonate is due to the higher experimental pH 8, compared to that for the other inorganic ligand experiments (pH 7). Our results are in line with Dragan et al. [52] who reported an inverse relationship between the logarithmic values of the association constant describing the binding of SYBR Green I to a DNA sequence and the dissolved NaCl concentration. These authors similarly ascribed their observations to a weakening of the electrostatic interactions between DNA and SYBR Green I with increasing ionic strength [54]. Although only $Na^+$ was considered as the counter cation, the ionic strength dependence shown in Fig. 5 should also apply to other ionic compositions encountered in natural waters.

The relative extents of the fluorescence intensity decrease with increasing SRFA concentration are comparable for the solution-based and hydrogel-supported DNA (Fig. 1F vs. 2F). Thus, in both cases, the observed effect of NDOM on fluorescence yield can be largely explained by the strong affinity of $Hg^{2+}$ for SRFA, which competes with the binding of $Hg^{2+}$ to the DNA. Strong complexation of $Hg^{2+}$ with natural organic matter is frequently observed in soils, sediments and aquatic environments, where $Hg^{2+}$-NDOM complexes often account for the majority of aqueous $Hg^{2+}$ species [47,55,56]. However, additional effects, including the weakening of electrostatic interactions and the hindering of the intercalation of SYBR Green I in the hairpin DNA structure, cannot be excluded at the higher SFRA concentrations (≥10 mg DOC $L^{-1}$) [52,57].

### 4.2. Performance of the DNA-functionalized hydrogel

The consistent agreements between the experimental data and the equilibrium calculations imply that the effects of variations in pH and ligand concentrations on the performance of the DNA-hydrogel sensor are due to the corresponding changes in $Hg^{2+}$ aqueous speciation and solution-DNA partitioning. For example, low pH and high $Cl^-$ concentrations reduce the binding of $Hg^{2+}$ to the DNA, resulting in a measurable fluorescence attenuation (Fig. 2A&B) [58]. The combined effect of pH and chlorinity can be seen for the Lake Superior ASW-I analog, where the acidic pH enhances the formation of Hg(II)-Cl complexes even at moderately low $Cl^-$ concentrations (Fig. 4A&B).

The strong affinity of NDOM toward $Hg^{2+}$ represents a major interference affecting the performance of the DNA-functionalized hydrogel sensor (Fig. 2F). In addition to the SRFA tested here, other types of NDOM, including humic acids and low molecular-weight organic acids, also have high complexation capacities toward $Hg^{2+}$ under a variety of natural conditions [55,57,59]. Because of the large heterogeneity in binding sites, NDOM poses a main challenge for the direct deployment of DNA-based $Hg^{2+}$ biosensors in the aquatic environments [56]. To account for the interferences, a quantitative description of the complexation reactions between $Hg^{2+}$ and NDOM is required, as illustrated by the speciation calculations in this study.

For a large number of natural waters, models such as the Humic Ion-Binding Model VII provide a means to estimate the binding of $Hg^{2+}$ to NDOM [48], if the relevant NDOM concentrations can be determined, for example with fluorescence methods

[60,61]. Tipping et al. [48,56] showed that the Humic Ion-Binding Model VII was able to explain the majority of published data on the binding of multiple metals, including $Hg^{2+}$, to NDOM from various sources. Likewise, our results of the SRFA experiments are also successfully reproduced by this model (Fig. 2F). It should be noted, however, that the parameter values describing $Hg^{2+}$ binding to NDOM in the Humic Ion-Binding Model VII are based on a relatively small and scattered number of published data from experiments with humic substances [56], and uncertainties are inevitably associated with these values.

The estimated $\Delta H_m$ for $Hg^{2+}$ complexation with the DNA indicates the reaction is exothermic, which in principle should result in less Hg(II)-DNA complex formation with increasing temperature. Complexation reactions of $Hg^{2+}$ with inorganic ligands (e.g., $OH^-$, $Cl^-$) [51,62] and organic ligands (e.g., cysteine) [63] are similarly exothermic. Overall, the effect of temperature turns out to be insignificant for samples with neutral and weakly alkaline pH (Fig. 3), because $Hg^{2+}$ speciation across the 5-50 ˚C range remains dominated by the Hg(II)-DNA complex.

## 5. Conclusions

In this study, we assessed two DNA-based sensing methods for the selective and fast detection of aqueous $Hg^{2+}$ under environmentally-relevant conditions. The performance of the first, solution-based DNA method is prone to environmental interferences that complicate the interpretation of the fluorescence measurements. The vulnerability of the solution DNA fluorescence to variable pH, ionic strength, and

SRFA concentrations is presumably due to their impacts on the interactions between the DNA and SYBR Green I molecules, as well as to the formation of stable complexes, including Hg(II)-Cl and Hg(II)-SRFA, that compete with the DNA for $Hg^{2+}$ binding. The solution-based DNA method could nonetheless be a sensitive and quick approach for aqueous $Hg^{2+}$ detection, if the measurements are conducted in a stable solution matrix, for example by using a pH 7 buffer solution and a relatively low sample to DNA-SYBR Green I solution volume ratio.

The second method immobilizes the DNA into a polyacrylamide hydrogel to monitor the selective binding of $Hg^{2+}$ to the DNA molecule outside of the sample matrix. While the DNA-functionalized hydrogel sensor largely eliminates the interferences observed for the solution-based DNA method, $Hg^{2+}$ complexation by $Cl^-$ and NDOM, when present at sufficiently high concentrations, may effectively compete with the DNA for $Hg^{2+}$. In addition, strongly acidic conditions and high temperatures (e.g., pH 3 and 40 ˚C) also attenuate the fluorescence yield of the DNA-functionalized hydrogel. However, the effects of pH, temperature and competing ligands can be accounted for by including the temperature-dependent $Hg^{2+}$ complexation constant to DNA derived in this study into equilibrium speciation calculations. This assumes, however, that information on the abundance and binding properties of the NDOM in the environment of interest can be obtained.

The DNA-functionalized hydrogel sensor is a promising tool for the detection of $Hg^{2+}$ in natural waters, especially in combination with routine monitoring of water quality

parameters, such as temperature, pH, conductivity and color, that help interpreting the sensor measurements. Although further testing is required, in particular to address the competitive binding of $Hg^{2+}$ to a wider range of NDOM, our results indicate that the DNA-functionalized hydrogel sensor performs well even in complex freshwater compositions like those of the Laurentian Great Lakes. The flexibility and stability of the hydrogel and the straightforward incorporation of the DNA sequence into the hydrogel support bode well for the engineering of environmental sensors that can be deployed for the fast, sensitive and high-resolution detection of aqueous $Hg^{2+}$ in the field.

## Supporting Material

Additional information and results are provided.

## Acknowledgements

We thank Dr. Shuhuan Li, Marianne Vandergriendt, Zijie Zhang and Dr. Po-Jung Jimmy Huang from the University of Waterloo for their valuable support in the laboratory. This research was financially supported by the Canada Excellence Research Chair (CERC) program to P.V.C., and the Strategic Partnership Grant for Project STPGP 507070 funded by the Natural Science and Engineering Research

Council of Canada to J.L..

## References

[1] C.T. Driscoll, R.P. Mason, H.M. Chan, D.J. Jacob, N. Pirrone, Mercury as a global pollutant: Sources, pathways, and effects, Environ. Sci. Technol., 47 (2013) 4967-4983.
[2] D. Durnford, A. Dastoor, D. Figueras-Nieto, A. Ryjkov, Long range transport of mercury to the Arctic and across Canada, Atmos. Chem. and Phys., 10 (2010) 6063-6086.
[3] W.F. Fitzgerald, D.R. Engstrom, C.H. Lamborg, C.-M. Tseng, P.H. Balcom, C.R. Hammerschmidt, Modern and historic atmospheric mercury fluxes in Northern Alaska: Global sources and arctic depletion, Environ. Sci. Technol., 39 (2005) 557-568.
[4] S.M. Ullrich, T.W. Tanton, S.A. Abdrashitova, Mercury in the aquatic environment: a review of factors affecting methylation, Crit. Rev. Environ. Sci. Technol., 31 (2001) 241-293.
[5] Q. Wang, D. Kim, D.D. Dionysiou, G.A. Sorial, D. Timberlake, Sources and remediation for mercury contamination in aquatic systems - a literature review, Environ. Pollut., 131 (2004) 323-336.
[6] N. Pirrone, S. Cinnirella, X. Feng, R.B. Finkelman, H.R. Friedli, J. Leaner, R. Mason, A.B. Mukherjee, G.B. Stracher, D.G. Streets, Global mercury emissions to the atmosphere from anthropogenic and natural sources, Atmos. Chem. and Phys., 10 (2010) 5951-5964.
[7] D.P. Krabbenhoft, E.M. Sunderland, Global change and mercury, Science, 341 (2013) 1457-1458.
[8] D. Mergler, H.A. Anderson, L.H.M. Chan, K.R. Mahaffey, M. Murray, M. Sakamoto, A.H. Stern, Methylmercury exposure and health effects in humans: a worldwide concern, AMBIO: A Journal of the Human Environment, 36 (2007) 3-11.
[9] WHO, Guideline for Drinking-Water Quality, 4th ed., World Health Organization. Geneva, Switzerland, (2011).
[10] P.M. Randall, S. Chattopadhyay, Mercury contaminated sediment sites - An evaluation of remedial options, Environ. Res., 125 (2013) 131-149.
[11] J. Wang, X. Feng, C.W. Anderson, Y. Xing, L. Shang, Remediation of mercury contaminated sites - A review, J. Hazard. Mater., 221-222 (2012) 1-18.
[12] F.X. Han, W.D. Patterson, Y. Xia, B.M. Sridhar, Y. Su, Rapid determination of mercury in plant and soil samples using inductively coupled plasma atomic emission spectroscopy, a comparative study, Water, Air, Soil Pollut., 170 (2006) 161-171.
[13] Z. Zhu, G.C.-Y. Chan, S.J. Ray, X. Zhang, G.M. Hieftje, Microplasma source based on a dielectric barrier discharge for the determination of mercury by atomic emission spectrometry, Anal. Chem., 80 (2008) 8622-8627.
[14] Y. Cai, Speciation and analysis of mercury, arsenic, and selenium by atomic fluorescence spectrometry, TrAC - Trends Anal. Chem., 19 (2000) 62-66.
[15] D. Sanchez-Rodas, W. Corns, B. Chen, P. Stockwell, Atomic fluorescence spectrometry: a suitable detection technique in speciation studies for arsenic, selenium, antimony and mercury, J. Anal. At. Spectrom., 25 (2010) 933-946.
[16] J. Chen, H. Chen, X. Jin, H. Chen, Determination of ultra-trace amount methyl-, phenyl-and inorganic mercury in environmental and biological samples by liquid chromatography with inductively coupled plasma mass spectrometry after cloud point extraction preconcentration, Talanta, 77 (2009) 1381-1387.
[17] X. Jia, Y. Han, X. Liu, T. Duan, H. Chen, Speciation of mercury in water samples by dispersive liquid-liquid microextraction combined with high performance liquid chromatography-inductively coupled plasma mass spectrometry, Spectrochim. Acta B, 66 (2011) 88-92.

[18] D. Martín-Yerga, M.B. González-García, A. Costa-García, Electrochemical determination of mercury: A review, Talanta, 116 (2013) 1091-1104.
[19] A.L. Suherman, E.E.L. Tanner, R.G. Compton, Recent developments in inorganic $Hg^{2+}$ detection by voltammetry, TrAC - Trends Anal. Chem., 94 (2017) 161-172.
[20] N. Dave, M.Y. Chan, P.-J.J. Huang, B.D. Smith, J. Liu, Regenerable DNA-functionalized hydrogels for ultrasensitive, instrument-free mercury(II) detection and removal in water, J. Am. Chem. Soc., 132 (2010) 12668-12673.
[21] P.-J.J. Huang, J. Liu, Sensing parts-per-trillion $Cd^{2+}$, $Hg^{2+}$, and $Pb^{2+}$ collectively and individually using phosphorothioate DNAzymes, Anal. Chem., 86 (2014) 5999-6005.
[22] P.-J.J. Huang, J. Lin, J. Cao, M. Vazin, J. Liu, Ultrasensitive DNAzyme beacon for lanthanides and metal speciation, Anal. Chem., 86 (2014) 1816-1821.
[23] J. Liu, Y. Lu, Rational design of "turn-on" allosteric DNAzyme catalytic beacons for aqueous mercury ions with ultrahigh sensitivity and selectivity, Angew. Chem., 119 (2007) 7731-7734.
[24] W. Zhou, R. Saran, J. Liu, Metal sensing by DNA, Chem. Rev., 117 (2017) 8272-8325.
[25] X.-B. Zhang, R.-M. Kong, Y. Lu, Metal ion sensors based on DNAzymes and related DNA molecules, Annu. Rev. Anal. Chem., 4 (2011) 105-128.
[26] S.B. Ebrahimi, D. Samanta, H.F. Cheng, L.I. Nathan, C.A. Mirkin, Forced intercalation (FIT)-aptamers, J. Am. Chem. Soc., 141 (2019) 13744-13748.
[27] A. Ono, H. Togashi, Highly selective oligonucleotide-based sensor for mercury(II) in aqueous solutions, Angew. Chem. Int. Ed., 43 (2004) 4300-4302.
[28] A.G. Memon, X. Zhou, J. Liu, R. Wang, L. Liu, B. Yu, M. He, H. Shi, Utilization of unmodified gold nanoparticles for label-free detection of mercury(II): Insight into rational design of mercury-specific oligonucleotides, J. Hazard. Mater., 321 (2017) 417-423.
[29] Z. Zhang, X. Fu, K. Li, R. Liu, D. Peng, L. He, M. Wang, H. Zhang, L. Zhou, One-step fabrication of electrochemical biosensor based on DNA-modified three-dimensional reduced graphene oxide and chitosan nanocomposite for highly sensitive detection of Hg(II), Sensors Actuators B: Chem., 225 (2016) 453-462.
[30] L. He, S. Zhang, M. Wang, D. Peng, F. Yan, Z. Zhang, L. Zhou, Facile fabrication of zinc phosphate-based nanocomposites for high-performance electrochemical sensing of Hg(II), Sensors Actuators B: Chem., 228 (2016) 500-508.
[31] Y. Tanaka, S. Oda, H. Yamaguchi, Y. Kondo, C. Kojima, A. Ono, $^{15}N$-$^{15}N$ J-coupling across $Hg^{II}$: Direct observation of $Hg^{II}$-mediated T-T base pairs in a DNA duplex, J. Am. Chem. Soc., 129 (2007) 244-245.
[32] Y. Miyake, H. Togashi, M. Tashiro, H. Yamaguchi, S. Oda, M. Kudo, Y. Tanaka, Y. Kondo, R. Sawa, T. Fujimoto, $Mercury^{II}$-mediated formation of thymine-$Hg^{II}$-thymine base pairs in DNA duplexes, J. Am. Chem. Soc., 128 (2006) 2172-2173.
[33] J. Wang, B. Liu, Highly sensitive and selective detection of $Hg^{2+}$ in aqueous solution with mercury-specific DNA and Sybr Green I, Chem. Commun., (2008) 4759-4761.
[34] K. Joseph, N. Dave, J. Liu, Electrostatically directed visual fluorescence response of DNA-functionalized monolithic hydrogels for highly sensitive $Hg^{2+}$ detection, ACS Appl. Mater. Inter., 3 (2011) 733-739.
[35] Y. Helwa, N. Dave, R. Froidevaux, A. Samadi, J. Liu, Aptamer-functionalized hydrogel microparticles for fast visual detection of mercury(II) and adenosine, ACS Appl. Mater. Inter., 4 (2012) 2228-2233.

[36] C.S. Kim, J.J. Rytuba, G.E. Brown Jr, EXAFS study of mercury(II) sorption to Fe- and Al-(hydr) oxides: I. Effects of pH, J. Colloid Interf. Sci., 271 (2004) 1-15.
[37] F.M. Morel, A.M. Kraepiel, M. Amyot, The chemical cycle and bioaccumulation of mercury, Annu. Rev. Ecol. Syst., 29 (1998) 543-566.
[38] W. Zhou, J. Ding, J. Liu, 2-Aminopurine-modified DNA homopolymers for robust and sensitive detection of mercury and silver, Biosens. Bioelectron., 87 (2017) 171-177.
[39] M. Stordal, G. Gill, L.S. Wen, P. Santschi, Mercury phase speciation in the surface waters of three Texas estuaries: Importance of colloidal forms, Limnol. Oceanogr., 41 (1996) 52-61.
[40] R.C. Averett, J.A. Leenheer, D.M. McKnight, K.A. Thorn, Humic substances in Suwannee River, Georgia: Interactions, properties and proposed structures, In: United States Geological Survey Water-Supply Paper 2373, 1995.
[41] J.A. Leenheer, J.P. Croue, Characterizing aquatic dissolved organic matter, Environ. Sci. Technol., 37 (2003) 18-26.
[42] J.A. Leenheer, Comprehensive approach to preparative isolation and fractionation of dissolved organic carbon from natural waters and wastewaters, Environ. Sci. Technol., 15 (1981) 578-587.
[43] S.R. Carpenter, N.F. Caraco, D.L. Correll, R.W. Howarth, A.N. Sharpley, V.H. Smith, Nonpoint pollution of surface waters with phosphorus and nitrogen, Ecol. Appl., 8 (1998) 559-568.
[44] S.C. Chapra, A. Dove, G.J. Warren, Long-term trends of Great Lakes major ion chemistry, J. Great Lakes Res., 38 (2012) 550-560.
[45] A. Dove, Long-term trends in major ions and nutrients in Lake Ontario, Aquat. Ecosyst. Health Manage., 12 (2009) 281-295.
[46] A. Dove, S.C. Chapra, Long-term trends of nutrients and trophic response variables for the Great Lakes, Limnol. Oceanogr., 60 (2015) 696-721.
[47] M. Ravichandran, Interactions between mercury and dissolved organic matter - a review, Chemosphere, 55 (2004) 319-331.
[48] E. Tipping, S. Lofts, J. Sonke, Humic Ion-Binding Model VII: a revised parameterisation of cation-binding by humic substances, Environ. Chem., 8 (2011) 225-235.
[49] W. Verweij, CHEAQS (a program for calculating CHemical Equilibria in AQuatic Systems). http://www.cheaqs.eu, (2018).
[50] D.L. Parkhurst, C.A.J. Appelo, Description of input and examples for PHREEQC version 3 - A computer program for speciation, batch-reaction, one-dimensional transport, and inverse geochemical calculations, U.S. Geological Survey Techniques and Methods, Book 6, Chap. A43, 497 pp. (2013).
[51] F. Di Natale, A. Erto, A. Lancia, D. Musmarra, Mercury adsorption on granular activated carbon in aqueous solutions containing nitrates and chlorides, J. Hazard. Mater., 192 (2011) 1842-1850.
[52] A.I. Dragan, R. Pavlovic, J.B. McGivney, J.R. Casas-Finet, E.S. Bishop, R.J. Strouse, M.A. Schenerman, C.D. Geddes, SYBR Green I: Fluorescence properties and interaction with DNA, J. Fluoresc., 22 (2012) 1189-1199.
[53] G. Cosa, K.S. Focsaneanu, J.R.N. McLean, J.P. McNamee, J.C. Scaiano, Photophysical properties of fluorescent DNA-dyes bound to single- and double-stranded DNA in aqueous buffered solution, Photochem. Photobiol., 73 (2001) 585-599.
[54] M.T. Record, C.F. Anderson, T.M. Lohman, Thermodynamic analysis of ion effects on the binding and conformational equilibria of proteins and nucleic acids: the roles of ion association or release, screening, and ion effects on water activity, Q. Rev. Biophys., 11 (2009) 103-178.
[55] W. Dong, L. Liang, S. Brooks, G. Southworth, B. Gu, Roles of dissolved organic matter in the

speciation of mercury and methylmercury in a contaminated ecosystem in Oak Ridge, Tennessee, Environ. Chem., 7 (2010) 94-102.
[56] E. Tipping, S. Lofts, H. Hooper, B. Frey, D. Spurgeon, C. Svendsen, Critical limits for Hg(II) in soils, derived from chronic toxicity data, Environ. Pollut., 158 (2010) 2465-2471.
[57] S. Han, G.A. Gill, Determination of mercury complexation in coastal and estuarine waters using competitive ligand exchange method, Environ. Sci. Technol., 39 (2005) 6607-6615.
[58] M.M. Kiy, A. Zaki, A.B. Menhaj, A. Samadi, J. Liu, Dissecting the effect of anions on $Hg^{2+}$ detection using a FRET based DNA probe, Analyst, 137 (2012) 3535-3540.
[59] C.L. Miller, G. Southworth, S. Brooks, L. Liang, B. Gu, Kinetic controls on the complexation between mercury and dissolved organic matter in a contaminated environment, Environ. Sci. Technol., 43 (2009) 8548-8553.
[60] N. Hudson, A. Baker, D. Reynolds, Fluorescence analysis of dissolved organic matter in natural, waste and polluted waters - a review, River Res. Appl., 23 (2007) 631-649.
[61] X. Lu, R. Jaffe, Interaction between Hg(II) and natural dissolved organic matter: A fluorescence spectroscopy based study, Water Res., 35 (2001) 1793-1803.
[62] C. Jeon, K.H. Park, Adsorption and desorption characteristics of mercury(II) ions using aminated chitosan bead, Water Res., 39 (2005) 3938-3944.
[63] M. Ngu-Schwemlein, J.K. Merle, P. Healy, S. Schwemlein, S. Rhodes, Thermodynamics of the complexation of Hg(II) by cysteinyl peptide ligands using isothermal titration calorimetry, Thermochim. Acta, 496 (2009) 129-135.

## Figure captions

**Figure 1.** Performance of solution-based DNA at 25 ˚C under variable solution pH (panel A), in the single inorganic ligand experiments (panels B-E), and in the presence of Suwannee River Fulvic Acid (SRFA, panel F).The results shown correspond to Exp. S-II to S-VII in Table 1.

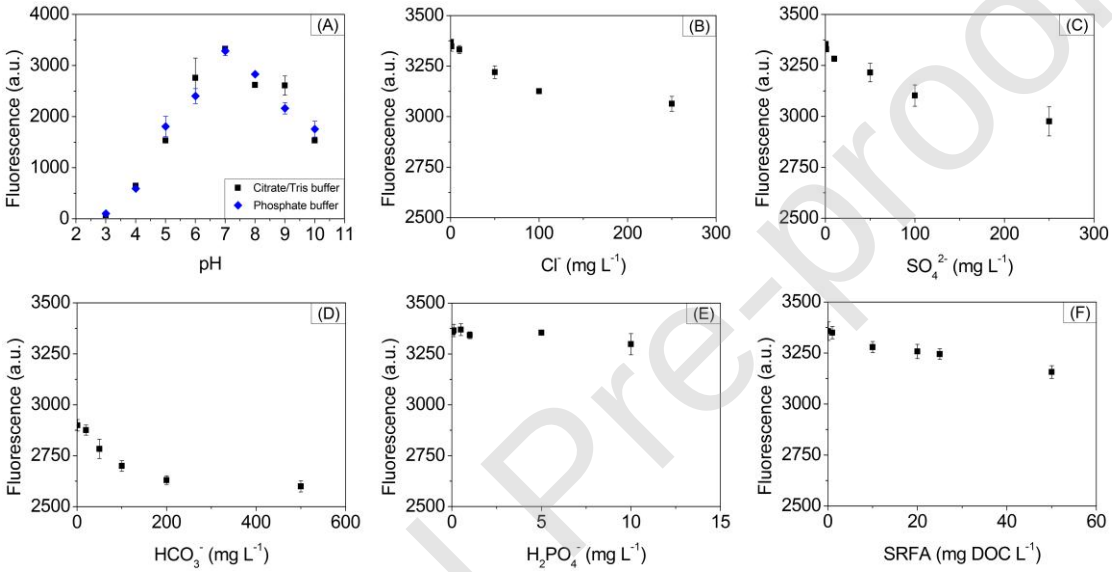


**Figure 2.** Performance of DNA-functionalized hydrogel at 25 ˚C under variable solution pH (panel A), in the single inorganic ligand experiments (panels B-E), and in the presence of Suwannee River Fulvic Acid (SRFA, panel F). The dashed lines show the distributions of the major $Hg^{2+}$ species derived from the equilibrium calculations; Hg(II)-DNA denotes the bridging complex between $Hg^{2+}$ and the DNA molecules and Hg(II)-SRFA the complexes between $Hg^{2+}$ and SRFA. The results shown correspond to Exp. G-II to G-VII in Table 1.

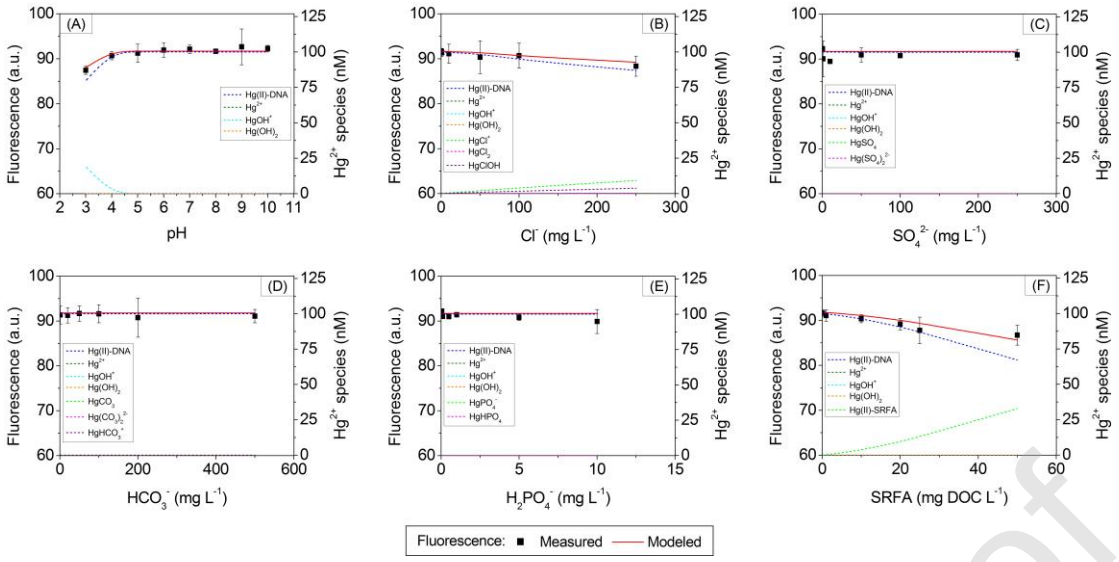


**Figure 3.** Performance of the DNA-functionalized hydrogel at variable solution temperature and three pH values (3, 7 and 9). The dashed lines show the distributions of the major $Hg^{2+}$ species derived from the equilibrium calculations; Hg(II)-DNA denotes the bridging complex between $Hg^{2+}$ and the DNA molecules. The results shown correspond to Exp. G-VIII in Table 1.

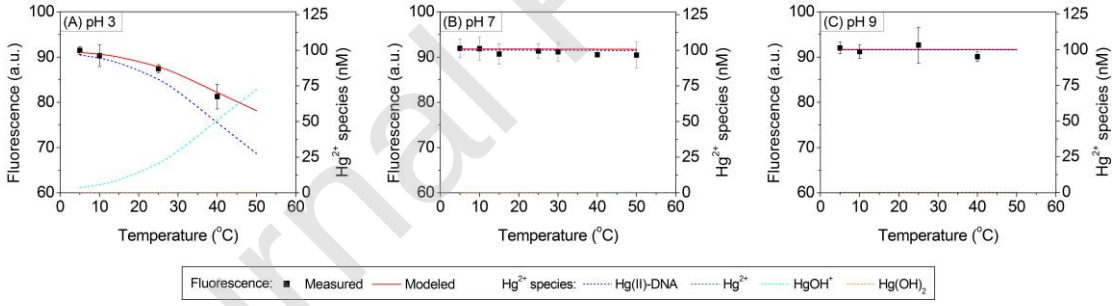


**Figure 4.** Fluorescence intensity detected by the DNA-functionalized hydrogel in the Laurentian Great Lakes analog solutions (ASW-I and ASW-II) spiked with 50 or 100 nM $Hg^{2+}$. ASW-I and ASW-II share the same inorganic compositions; ASW-II solutions additionally contain 10 mg DOC $L^{-1}$ of Suwannee River Fulvic Acid (SRFA). The dashed lines show the distributions of the major $Hg^{2+}$ species derived from the equilibrium calculations; Hg(II)-DNA denotes the bridging complex between $Hg^{2+}$

and the DNA molecules and Hg(II)-SRFA the complexes between $Hg^{2+}$ and SRFA. The results shown correspond to Exp. G-IX and G-X in Table 1.

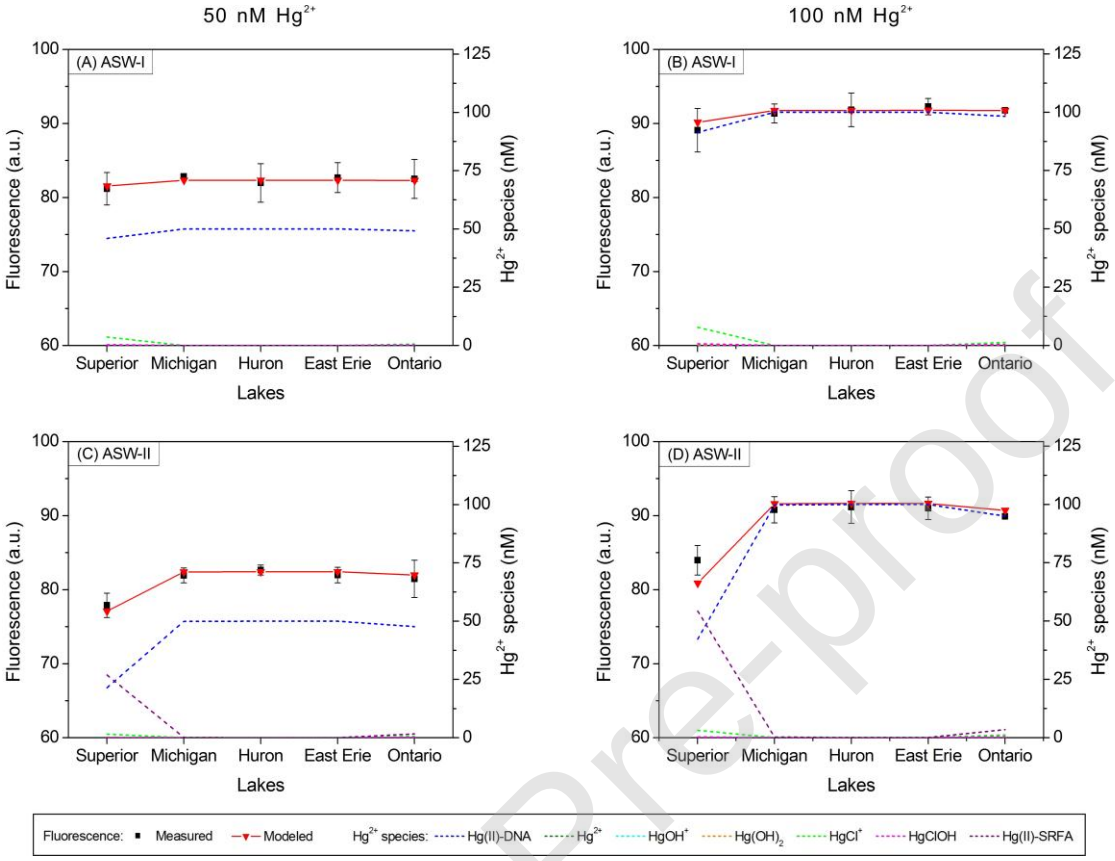


**Figure 5.** Fluorescence intensity versus ionic strength in the solution-based DNA experiments with inorganic ligands added. The results shown correspond to Exp. S-III to S-VI in Table 1. The solid lines are exponential fits to the measured data.

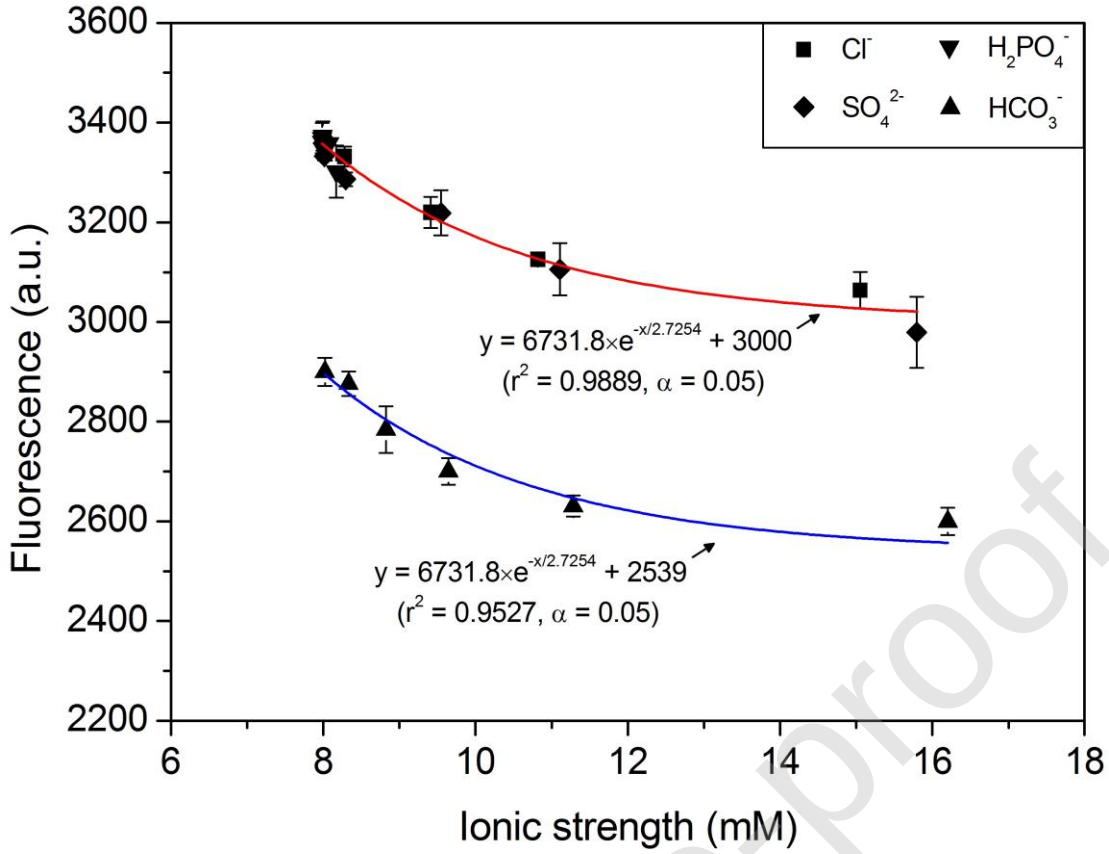

## Table captions

**Table 1** Summary of experimental design.

| **Solution-based DNA** | | | | | | | |
|---|---|---|---|---|---|---|---|
| | $Hg^{2+}$ (nM) | DNA (nM) | SYBR Green I (nM) | pH [a] | Inorganic ligands (mg $L^{-1}$) | SRFA [b] (mg DOC $L^{-1}$) | Temperature (˚C) |
| Exp. S-I [c] | 10 - 500 | 100 | 600 | 7 | - | - | 25 |
| Exp. S-II | 90 | 100 | 600 | 3 - 10 | - | - | 25 |
| Exp. S-III | 90 | 100 | 600 | 7 | $Cl^-$: 0.5 - 250 | - | 25 |
| Exp. S-IV | 90 | 100 | 600 | 7 | $SO_4^{2-}$: 0.5 - 250 | - | 25 |
| Exp. S-V | 90 | 100 | 600 | 8 | $HCO_3^-$: 1 - 500 | - | 25 |
| Exp. S-VI | 90 | 100 | 600 | 7 | $H_2PO_4^-$: 0.05 - 10 | - | 25 |
| Exp. S-VII | 90 | 100 | 600 | 7 | - | 0.1 - 50 | 25 |
| **DNA-functionalized hydrogel** | | | | | | | |
| | $Hg^{2+}$ (nM) | DNA (nM) | SYBR Green I (nM) | pH [a] | Inorganic ligands (mg $L^{-1}$) | SRFA [b] (mg DOC $L^{-1}$) | Temperature (˚C) |
| Exp. G-I [d] | 10 - 500 | 3000±20 | 610 | 7 | - | - | 25 |
| Exp. G-II | 100 | 3000±20 | 610 | 3 - 10 | - | - | 25 |
| Exp. G-III | 100 | 3000±25 | 610 | 7 | $Cl^-$: 0.5 - 250 | - | 25 |
| Exp. G-IV | 100 | 3000±22 | 610 | 7 | $SO_4^{2-}$: 0.5 - 250 | - | 25 |
| Exp. G-V | 100 | 3000±20 | 610 | 8 | $HCO_3^-$: 1 - 500 | - | 25 |
| Exp. G-VI | 100 | 3000±20 | 610 | 7 | $H_2PO_4^-$: 0.05 - 10 | - | 25 |
| Exp. G-VII | 100 | 3000±25 | 610 | 7 | - | 0.1 - 50 | 25 |

| | | | | | | | |
|---|---|---|---|---|---|---|---|
| Exp. G-VIII | 100 | 3000±23 | 610 | 3, 7, 9 | - | - | 5 - 50 |
| Exp. G-IX | 50, 100 | 3000±25 | 610 | ASW-I (no SRFA) [e] | | | 25 |
| Exp. G-X | 50, 100 | 3000±25 | 610 | ASW-II (SRFA 10 mg DOC $L^{-1}$) [e] | | | 25 |

Notes: [a] pH buffers used: pH 3-6, 8 mM sodium citrate, and pH 7-10, 8 mM Tris nitrate; in addition, in Exp. S-II the following buffer was also used for comparison: pH 3-10, 8 mM sodium phosphate; [b] Suwannee River Fulvic Acid (SRFA) used as a proxy of DOM in natural waters; [c] Used to derive the calibration curve for the solution-based DNA sensing method; [d] Used to build the calibration curve for the hydrogel-based sensor; [e] Artificial surface water type I (ASW-I) was prepared based on the hydrochemistry of the Great Lakes given in Table 2 and ASW-II prepared by adding SRFA with a final concentration of 10 mg DOC $L^{-1}$ to ASW-I.

**Table 2** Representative hydrochemistry of the Laurentian Great Lakes used in Exp. G-IX and G-X in Table 1.

| Lake | pH | $Na^+$ [a] (mg $L^{-1}$) | $K^+$ (mg $L^{-1}$) | $Ca^{2+}$ (mg $L^{-1}$) | $Mg^{2+}$ (mg $L^{-1}$) | $Cl^-$ (mg $L^{-1}$) | $SO_4^{2-}$ (mg $L^{-1}$) | Alkalinity (mg $CaCO_3$ $L^{-1}$) | $NO_3^-$ (mg $L^{-1}$) | Total P (mg P $L^{-1}$) |
|---|---|---|---|---|---|---|---|---|---|---|
| Superior | 6.3 | 1.38 | 0.51 | 13.62 | 2.83 | 1.42 | 3.85 | 41.9 | 1.73 | 0.003 |
| Michigan | 7.5 | 6.02 | 1.41 | 35.95 | 11.28 | 12.05 | 24.01 | 107.9 | 1.46 | 0.003 |
| Huron | 8.3 | 3.57 | 0.94 | 26.40 | 7.46 | 6.58 | 15.83 | 78.5 | 1.64 | 0.004 |
| East Erie | 8.2 | 7.16 | 1.43 | 32.11 | 8.89 | 14.58 | 22.81 | 88.9 | 1.15 | 0.009 |
| Ontario | 6.9 | 11.41 | 1.50 | 33.55 | 8.61 | 19.56 | 25.54 | 90.1 | 2.04 | 0.004 |

Notes: [a] $Na^+$ concentration was adjusted to achieve charge balance in the PHREEQC-3 calculations.